



Nanostructured $\text{Fe}_2\text{O}_3/\text{TiO}_2$ thick films prepared by screen printing[#]

Obrad S. Aleksic¹, Zorka Z. Djuric², Maria V. Nikolic^{1,*}, Nikola Tasic¹, Marina Vukovic¹, Zorica Marinkovic-Stanojevic¹, Nenad Nikolic¹, Pantelija M. Nikolic²

¹Institute for Multidisciplinary Research, University of Belgrade, Kneza Visislava 1, 11000 Belgrade, Serbia

²Institute of Technical Sciences of SASA, Knez Mihailova 35, 11000 Belgrade, Serbia

Received 12 June 2013; received in revised form 27 August 2013; accepted 12 September 2013

Abstract

Nanostructured single layered (pure TiO_2 , pure $\alpha\text{-Fe}_2\text{O}_3$ and mixed $\text{Fe}_2\text{O}_3/\text{TiO}_2$ with two different oxide ratios, 2 : 3 and 3 : 2) and double layered (TiO_2 layer over a Fe_2O_3 layer) thick films have been fabricated by screen printing technology on a glass substrate. The pastes used for film preparation were obtained by adding an organic vehicle to the oxide powders together with a small percentage of binding glass frit. Samples were dried up to 100 °C and sintered at 650 °C/60 minutes. Structural, morphological and optical studies have been carried out using XRD, SEM analyses and UV/Vis spectroscopy. The prepared pure and mixed $\text{Fe}_2\text{O}_3/\text{TiO}_2$ thick films had a homogenous nanostructure without secondary phases. Indirect band gaps were determined from the measured transmission spectra and the obtained values are in the range of literature data.

Keywords: nanostructures, thick films, screen printing, microstructure, optical properties

I. Introduction

Significant modifications of the properties of bulk materials provided by nanosized materials have opened many new fields of applications. One field of application is in photoelectrochemical cells. New generation photovoltaic cells are based on nanocrystalline materials and conducting polymer films [1]. Nanostructured materials are also optimal candidates for gas sensing [2].

Nanostructured titania (TiO_2) films are widely applied as photovoltaic solar cells, photovoltaic reactors, high performance anodes in ion batteries, gas sensors, electrochromic displays and electrical insulators [2,3].

Hematite ($\alpha\text{-Fe}_2\text{O}_3$) is a low cost, naturally abundant, stable material that has many potential applications [4]. Some of the limitations of hematite in view of application as a photoelectrochemical anode can be overcome using nanostructures. Another approach to improving the properties of hematite is elemental doping with dopants such as Ti, Sn, Si [5,6].

Thick film technology offers the possibility of producing high performance devices at a very low cost [3]. Because of that, in this work we have fabricated nanostructured single layered (pure TiO_2 , pure $\alpha\text{-Fe}_2\text{O}_3$ and mixed $\text{Fe}_2\text{O}_3/\text{TiO}_2$ with two different oxide ratios, 2 : 3 and 3 : 2) and double layered (TiO_2 layer over a Fe_2O_3 layer) thick films by screen printing on a glass substrate. Structural, morphological and optical studies have been carried out.

II. Experimental

Starting powders of TiO_2 (Alfa Aesar, 99.7% anatase, grain size 15 nm) and $\alpha\text{-Fe}_2\text{O}_3$ (Alfa Aesar, 99%, grain size 20–60 nm) were used. The two oxide mixtures (40% $\alpha\text{-Fe}_2\text{O}_3$ / 60% TiO_2 and 60% $\alpha\text{-Fe}_2\text{O}_3$ / 40% TiO_2) were homogenized in a planetary ball mill (Fritsch Pulverisette 5) in stainless steel bowls with stainless steel balls for 60 min. Four thermistor pastes were made by mixing the initial starting powders (TiO_2 and $\alpha\text{-Fe}_2\text{O}_3$) or oxide mixtures (40% $\alpha\text{-Fe}_2\text{O}_3$ / 60% TiO_2 and 60% $\alpha\text{-Fe}_2\text{O}_3$ / 40% TiO_2) with an organic vehicle (butyl cellulose) and a small amount of binding lead boron silicon oxide glass frit to improve adhesion to the substrate. The pastes were screen printed on a glass substrate and five different thick films were prepared (Table 1). Samples were dried up to 100 °C and

[#] Paper presented at 2nd Conference of The Serbian Ceramic Society - 2CSCS-2013, Belgrade, Serbia, 2013

* Corresponding author: tel: +381 11 202 7284
e-mail: mariav@rcub.bg.ac.rs

Table 1. Composition and notation of prepared thick films

Sample notation	Composition	$\alpha\text{-Fe}_2\text{O}_3$ [wt.%]	TiO_2 [wt.%]
TO	TiO_2	0	100
FO	$\alpha\text{-Fe}_2\text{O}_3$	100	0
40FO/60TO	40% $\alpha\text{-Fe}_2\text{O}_3$ / 60% TiO_2	40	60
60FO/40TO	60% $\alpha\text{-Fe}_2\text{O}_3$ / 40% TiO_2	60	40
TO@FO	bi-layered $\text{TiO}_2/\alpha\text{-Fe}_2\text{O}_3$ film	100*	100**

* the first layer, ** the second layer

then fired at 650 °C/60 minutes in a hybrid conveyor furnace in air. XRD analysis of the samples was performed on a Rigaku RINT 2000 device. SEM analysis was performed on a TESCAN Electron Microscope VEGA TS 5130MM. Transmittance was measured on a UV/Vis Shimadzu UV-2600 with an ISR2600Plus Integrating sphere attachment in the measuring range 220–1400 nm. Baseline correction was made using the glass plate substrate.

III. Results and discussion

XRD diagrams of thick film samples are shown in Fig. 1. Three phases were noted: hematite, according to JCPDS card 89-8104, rhombohedral space group $R3c$ (167), anatase, according to JCPDS card 89-4921, tetragonal space group $I4_1/amd$ (141) and rutile, according to JCPDS card 89-4920, tetragonal space group $P4_2/mnm$ (136) in the thick films of oxide mixtures (40% $\alpha\text{-Fe}_2\text{O}_3$ / 60% TiO_2 and

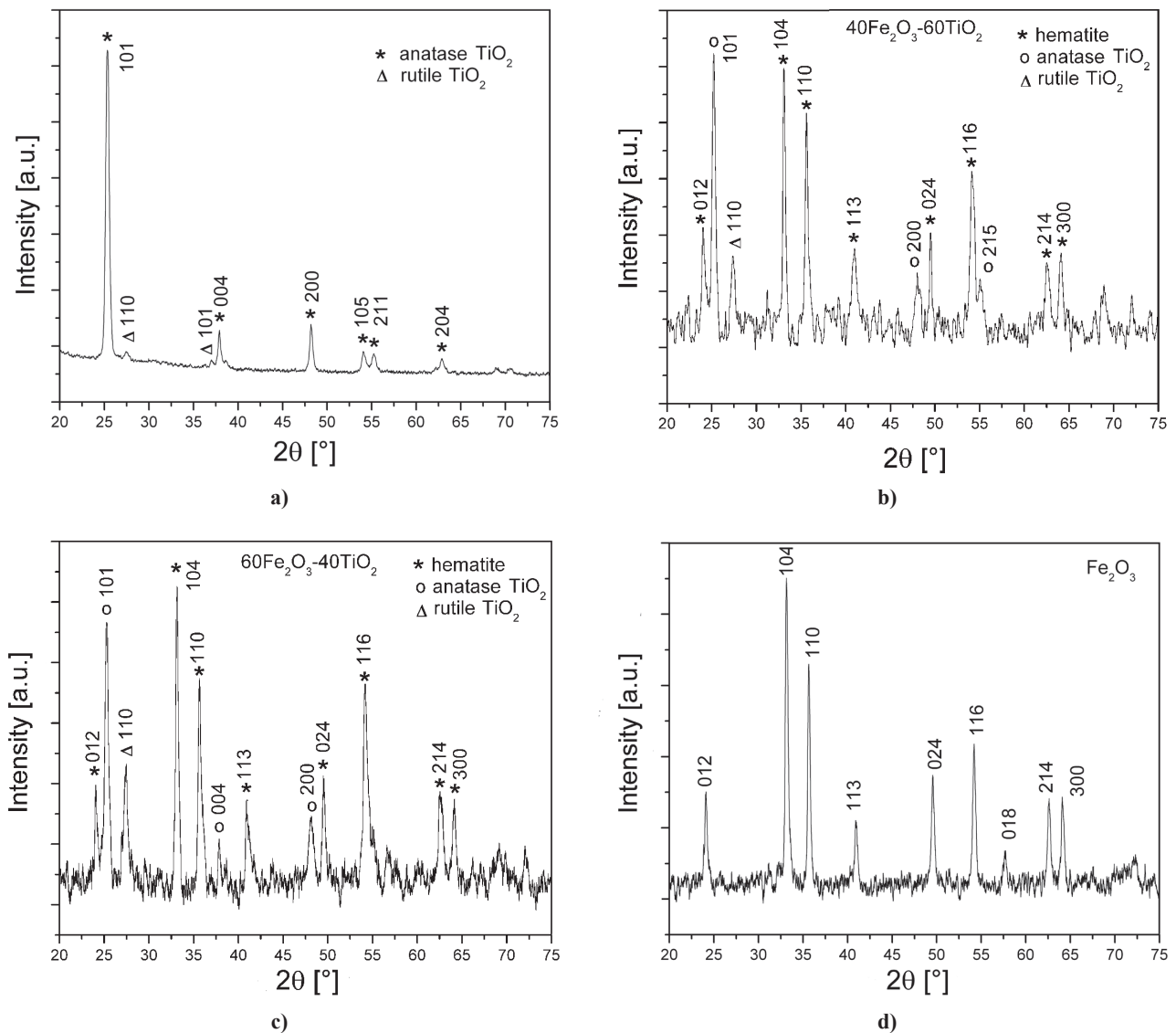


Figure 1. XRD diffractograms of prepared thick films: a) TO, b) 40FO/60TO, c) 60FO/40TO and d) FO

60% α -Fe₂O₃ / 40% TiO₂), while the hematite FO thick film contained only this phase, and the TO thick film contained anatase and rutile phases. As the sintering temperature of the thick films was low (650 °C) and below the irreversible transformation temperature of anatase to rutile of 700 °C [3], the anatase phase was the dominant TiO₂ phase especially in the TO thick film. Slightly more rutile was present in the thick films made of oxide mixtures that can be the result of ho-

mogenization of starting powders combined with subsequent sintering.

SEM micrographs of the thick film samples show that all films were homogenous, with relatively small grains, agglomerates and porosity typical of thick films. Figures 2a,b,c,d shows the surface and cross-section of the TO and FO thick films. The thickness of the film samples was estimated to be between 10 and 15 μ m. The pure TiO₂ thick films are slightly coars-

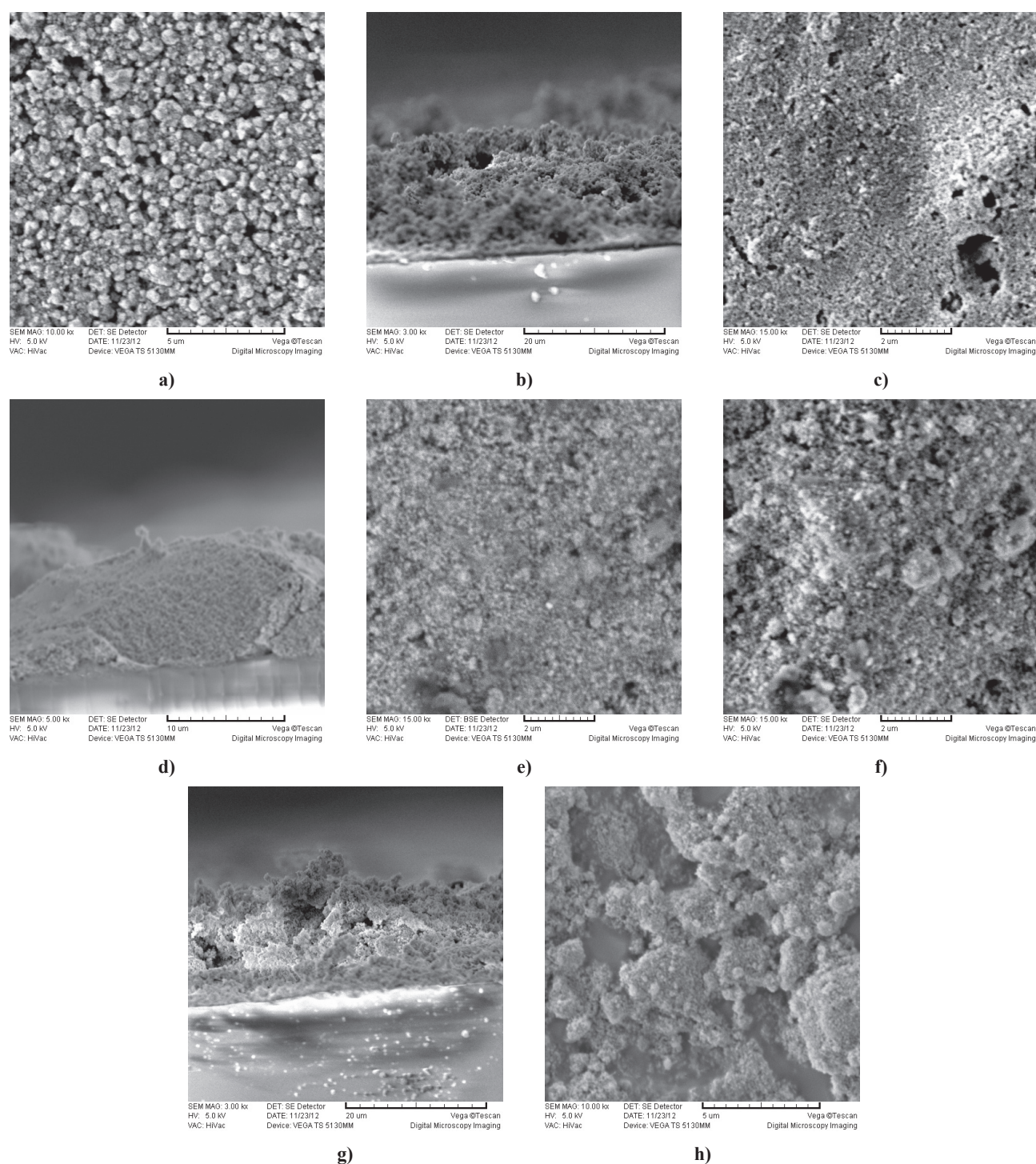


Figure 2 SEM micrographs of prepared thick films: TO (surface (a), cross-section (b)); FO (surface (c) and cross-section (d)); 40FO/60TO (surface in back scattering electrons (BSE) mode (e) and secondary electron (SE) mode (f)); and 60FO/40TO (cross-section (g) and surface (h))

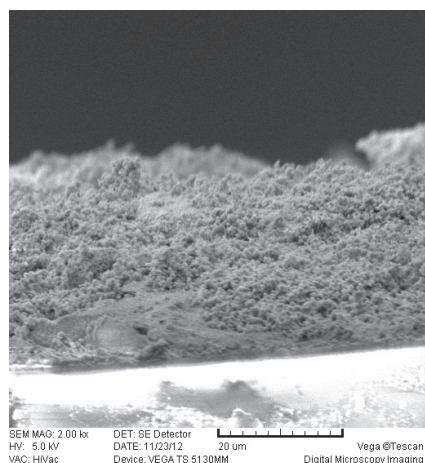


Figure 3. SEM micrograph of TO@FO (bi-layered $\text{Fe}_2\text{O}_3/\text{TiO}_2$) thick film – cross section

er, with more agglomerates even though the sintering temperature was low. Grain-size increase due to coalescence of grains has previously been noticed for TiO_2 thin [2] and thick [3,7] films. The pure hematite FO thick films retained the fine small grain structure of starting powders. Both thick films made of oxide mixtures (40% $\alpha\text{-Fe}_2\text{O}_3$ / 60% TiO_2 and 60% $\alpha\text{-Fe}_2\text{O}_3$ / 40% TiO_2) had a homogenous structure with small grains as shown on Figs. 2e,f,g,h. The grain size was slightly larger than for the pure hematite thick films, but smaller than for the pure titania TO thick films. Inhibition of grain growth suffered by titania nanograins through addition of iron oxide was noted by Comini *et al.* [8] in the case of the titanium and iron oxide nanosized thin films. Such a structure enables possible application of the obtained mixed oxide thick films as gas sensors.

Figure 3 shows the cross section of the TO@FO sample (bi-layered $\text{Fe}_2\text{O}_3/\text{TiO}_2$ thick film). As the TiO_2 layer was screen printed over the $\alpha\text{-Fe}_2\text{O}_3$ layer the film thickness was estimated to be about 30 mm.

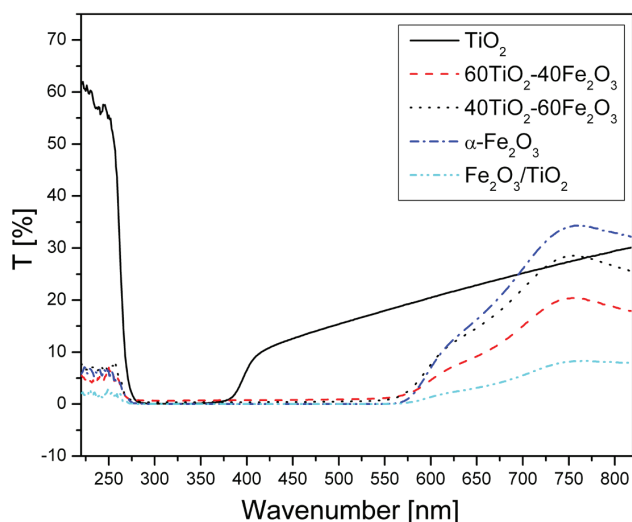


Figure 4. Transmittance spectra of TO, FO, 40FO/60TO, 60FO/40TO and TO@FO thick film samples

Figure 4 shows the transmittance spectra measured for the analysed thick film samples. The absorption coefficient was calculated from measured transmission values using the UV-Probe software. The optical band gaps of the investigated thick films can be estimated using Tauc plots that relate the absorption coefficient with the density of optically absorbing energy transitions within a semiconductor [9]. The relationship of Davis and Mott [10] was used where, $\alpha = [A(h\nu - E_g)^m]/(h\nu)$, where A is a constant related to the density of electronic states above and below the band gap, $h\nu$ is the absorbed photon energy and E_g is the optical band gap relating to direct allowed transitions, when $m = 1/2$ and indirect phonon assisted transitions, when $m = 2$. For titania TO thick films the indirect band gap energy was determined as 2.99 eV, as shown in Fig. 5a. This was in accordance with the literature values [7,11]. The indirect band gap determined for the FO thick film was 2.05 eV, as shown in Fig. 5b, that is in the range of the determined literature data for hematite [5,12]. For the mixed oxides, the indirect band gap energies determined for the 40FO/60TO and 60FO/40TO thick films was 1.92 eV and 1.99 eV, respectively, while the determined direct band gap energies were 1.97 and 2.04, respectively. These values were in the range of the determined literature values for hematite, taking into account the differences reported for crystalline and nanocrystalline $\alpha\text{-Fe}_2\text{O}_3$ thin films, concerning the influence of the film thickness and grain structure on optical properties [13,14].

IV. Conclusions

In this work single layered (pure TiO_2 , pure $\alpha\text{-Fe}_2\text{O}_3$ and mixed $\text{Fe}_2\text{O}_3/\text{TiO}_2$ with two different oxide ratios, 2 : 3 and 3 : 2) and double layered (TiO_2 layer over a Fe_2O_3 layer) thick films on a glass substrate were fabricated using starting nanopowders of TiO_2 (mostly anatase) and $\alpha\text{-Fe}_2\text{O}_3$ and screen printing technology. The deposited films were sintered at 650 °C/60 minutes. Structural (XRD) and morphological (SEM) studies revealed homogenous thick films with a small grain size and thickness between 10 and 15 mm for the single layered and about 30 mm for the bi-layered films. The optical band gap was determined from measured transmission spectra, and for the mixed oxide thick films was in the literature range of pure and doped hematite. This initial research confirms possible wide applicability of the fabricated thick films. Further research will involve a detailed analysis of a wide range of properties of thick films made of the fabricated mixed oxide thick film pastes on different substrates such as alumina and fluorine-tin-oxide coated glass.

Acknowledgements: This work was performed as part of project III45007 financed by the Ministry for Edu-

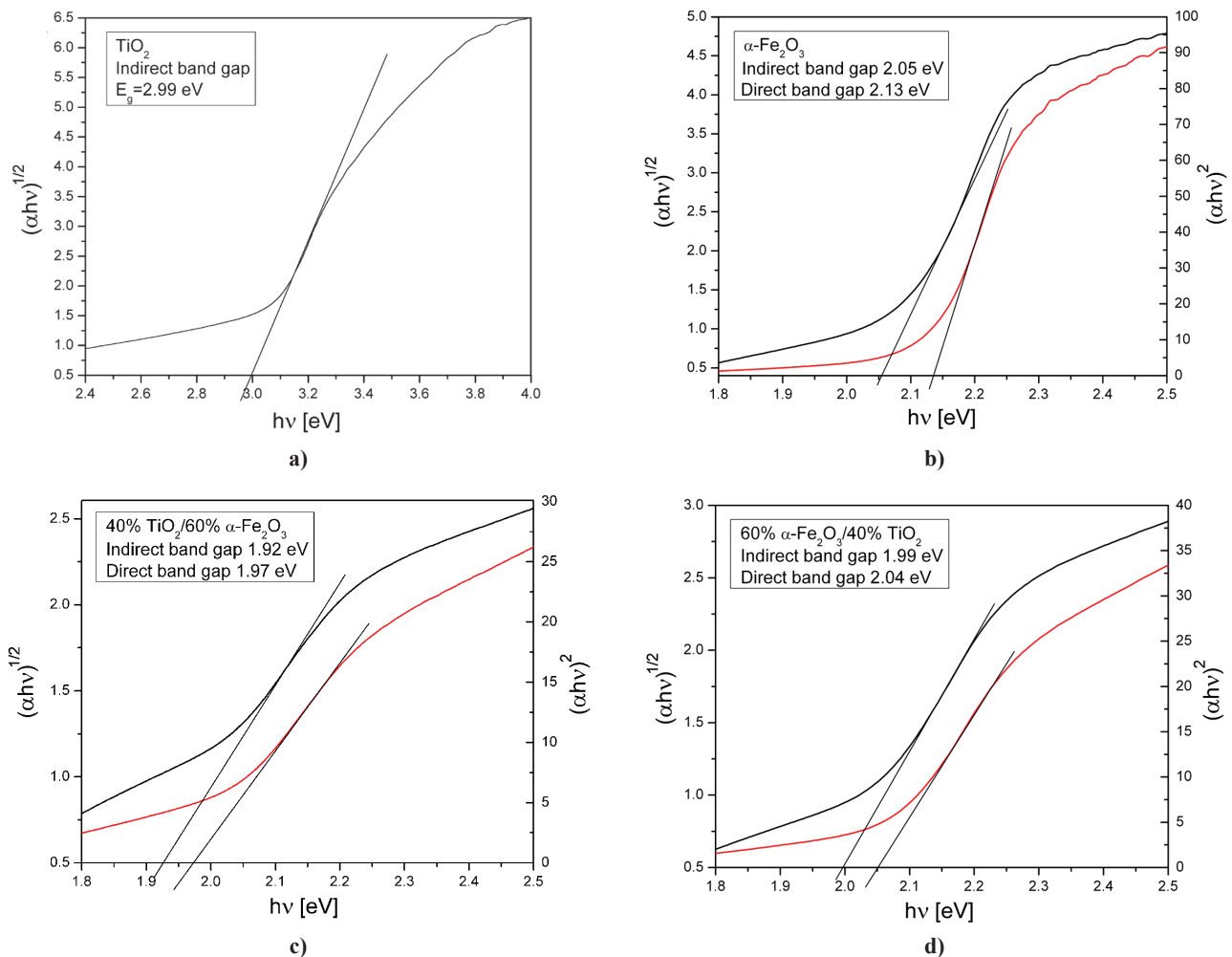


Figure 5. Direct and indirect Tauc plots of thick films: a) TO, b) FO, c) 40FO/60TO and d) 60FO/40TO

cation, Science and Technological Development of the Republic of Serbia.

References

1. M. Graetzel, "Photoelectrochemical cells", *Nature*, **414** (2001) 338–344.
2. E. Comini, V. Guidi, C. Frigeri, I. Ricco, G. Sberveglieri, "CO sensing properties of titanium and iron oxide nanosized thin films", *Sensor Actuat. B - Chem.*, **77** (2001) 16–21.
3. M.C. Carotta, M. Ferroni, V. Guidi, G. Martinelli, "Preparation and characterization of nanostructured titania thick films", *Adv. Mater.*, **11** [11] (1999) 943–946.
4. D.A. Wheeler, G.M. Wang, Y.C. Ling, Y. Li, J.Z. Zhang, "Nanostructured hematite: synthesis, characterization, charge carrier dynamics and photoelectrochemical properties", *Energy Environ. Sci.*, **5** (2012) 6682–6702.
5. M.L. Zhang, W.J. Luo, Z.S. Li, Z.G. Zou, "Improved photoelectrochemical responses of Si and Ti codoped α -Fe₂O₃ photoanode films", *Appl. Phys. Lett.*, **97** (2010) 042105.
6. N.T. Hahn, C.B. Mullins, "Photoelectrochemical performance of nanostructured Ti- and Sn-doped α -Fe₂O₃ photoanodes", *Chem. Mater.*, **22** (2010) 6474–6482.
7. M. Bonini, M.C. Carotta, A. Chiorino, V. Guidi, C. Malagu, G. Martinelli, L. Paglialonga, M. Sacerdoti, "Doping of nanostructured titania thick film: structural and electrical investigations", *Sensor Actuat. B - Chem.*, **68** (2000) 274–280.
8. E. Comini, G. Sberveglieri, M. Ferroni, V. Guidi, C. Frigeri, D. Boscarino, "Production and characterization of titanium and iron oxide nano-sized thin films", *J. Mater. Res.*, **16** [6] (2001) 1559–1564.
9. D.L. Wood, J. Tauc, "Weak absorption tails in amorphous semiconductors", *Phys. Rev. B*, **5** (1972) 3144–3151.
10. E.A. Davis, N.F. Mott, "Conduction in non-crystalline systems. V. Conductivity, optical absorption and photoconductivity in amorphous semiconductors", *Philos. Mag.*, **22** (1970) 903–922.
11. J. Pascual, J. Camassel, H. Mathieu, "Fine structure in the intrinsic edge of TiO₂", *Phys. Rev. B*, **18** [10] (1978) 5606–5614.
12. J.A. Glasscock, P.R.F. Barnes, I.C. Plumb, A. Ben-david, P.J. Martin, "Structural, optical and electrical properties of undoped polycrystalline hematite thin films produced using filtered arc deposition", *Thin Solid Films*, **516** (2008) 1716–1724.

13. J.A. Glasscock, P.R.F. Barnes, I.C. Plumb, N. Savvides, “Enhancement of photoelectrochemical hydrogen production from hematite thin films by the introduction of Ti and Si”, *J. Phys. Chem. C*, **111** (2007) 16477–16488.
14. A.A. Akl, “Optical properties of crystalline and non-crystalline iron oxide thin films deposited by spray pyrolysis”, *Appl. Surf. Sci.*, **233** (2004) 307–319.